ATMOSPHERIC RESEARCH

RECHERCHE ATMOSPHÉRIQUE

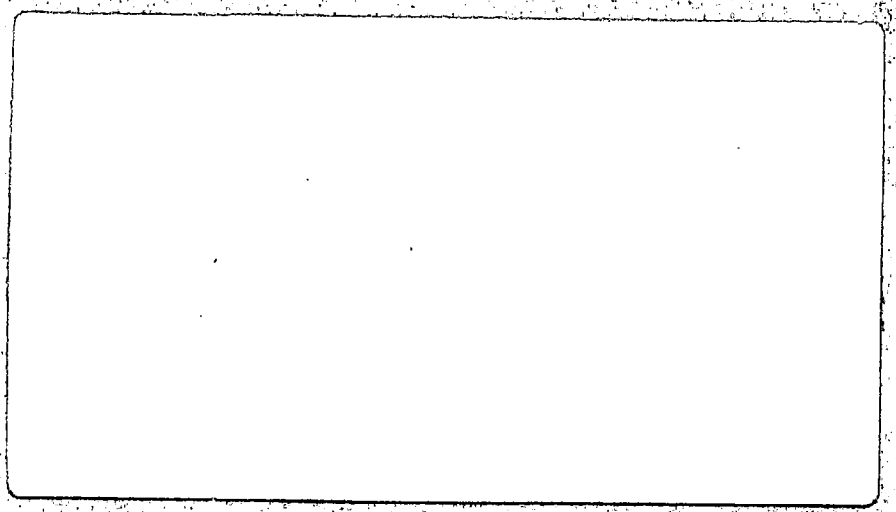

ATMOSPHERIC ENVIRONMENT

ENVIRONNEMENT ATMOSPHÉRIQUE

Report - ARQL - 77/9 August 1977

Experiments with a one-dimensional time-dependent planetary boundary layer model

GUILLERMO BERRI

National Meteoroloical Service
Buenos Aires - Argentina

This is one of a series of internal reports prepared by the Atmospheric Research Directorate.

The views expressed in this document reflect the opinion of the individual contributor and do not necessarily represent the official position of the Atmospheric Environment Service.

It should not be referenced or quoted without the written permission of the author.

This study was carried out while the author was a visiting WMO Fellow.

Air Quality and Inter-Environmental Research Branch
Atmospheric Environment Service
4905 Dufferin Street
Downsview, Ontario
M3H 5T4

TABLE OF CONTENTS

ABSTRACT

A one-dimensional time-dependent PBL model is investigated. The model is based on the primitive equations with an eddy diffusivity closure for the turbulent fluxes of heat and momentum. Within the surface layer the constraints of Monin-Obukhov similarity theory are imposed. Surface heat flux is specified as the positive half cycle of a diurnal sinusoid. At the upper boundary, a strong inversion, a downward heat flux with 20% of the surface value is imposed. Predictions of the model are compared with observations from the Great Plains Experiment, O'Neill, Nebraska, 25 August 1953. The comparison shows good general agreement.

ACKNOWLEDGEMENTS

The author is gratefully indebted to Drs. J. Walmsley and J. Reid of the Boundary Layer Research Division (A.E.S.), for the great assistance and useful comments throughout the project and also for kindly revising this report; also to Dr. C. Matthias for his useful suggestions. The author wishes to thank all the members of the staff of the Air Quality and Inter-Environmental Research Branch, through its Director, Dr. M. Kwizak, for their assistance, and especially Mr. J. McLernon for his hospitality and coordination of the fellowship.

Finally the author wishes to thank very much Mrs. P. Pearson, who kindly typed this report.

This research project was supported through a WMO-UNEP fellowship.

1. INTRODUCTION

The author was granted a nine month WMO-UNEP fellowship for Air Pollution Meteorology Studies at the Atmospheric Environment Service (A.E.S.) Downsview, Ontario, CANADA. The last six months of that period were dedicated to a research project on numerical modeling of the Planetary Boundary Layer for use in Air Pollution Meteorology studies.

The main purpose is to experiment with a simple one-dimensional time-dependent Planetary Boundary Layer model, suitable for Air Pollution Meteorology studies.

Most of the sources of air pollutants are confined in the first tens of meters just above the earth's surface. Once the pollutants are emitted to the air, their diffusion and transport is determined by the atmospheric characteristics inside the PBL.

The a priori limitations imposed by the assumption of horizontal homogeneity restrict the field of application of such models, although a good resolution of the vertical structure of the PBL can give a good estimation of the atmospheric diffusion capacity.

The author interprets that this is a necessary first step toward more elaborate models capable of studying specific cases like local circulations induced by horizontal inhomogeneity.

II THE MODEL

2.1 Governing Equations

Basically, the model consists of the solution of the two horizontal momentum equations and the thermodynamic equation:

$$\frac{\partial u_i}{\partial t} + u_j \frac{\partial u_i}{\partial x_j} = -\frac{1}{\rho}\frac{\partial p}{\partial x_i} - g\,\delta_{3i} + \nu \frac{\partial^2 u_i}{\partial x_j^2} - \varepsilon_{ijk} f_j u_k \qquad (2.1.1)$$

$$\frac{\partial \theta}{\partial t} + u_j \frac{\partial \theta}{\partial x_j} = \chi_T \frac{\partial^2 \theta}{\partial x_j^2} \qquad (2.1.2)$$

where the explanation of the symbols can be found in the appendix.

Equation (2.1.1) are the three components of the Navier-Stokes equations, expressed as one equation in tensor form, showing respectively the net force applied to an element of fluid equal to the pressure and gravity forces, the molecular diffusivity of momentum and the coriolis force, all per unit of mass. Equation (2.1.2), the thermodynamic equation, shows the total variation of the potential temperature equal to the molecular thermal diffusivity.

Already neglected in the last equation is the term involving the latent heat release, of the form $(L_v\theta/c_pT)dq_s/dt$, because this model does not include humidity. Also neglected is the divergence of the radiative flux, of the form $(1/\rho c_p)\partial R_j/\partial x_j$, because the behaviour of this term is not well known yet and according to Busch (1973) can be neglected for heights greater than 2 meters above the earth's surface. This can be

one of the sources of inaccuracy in dealing with the thermodynamic equation. In equation (2.1.1) the term $\nu\, \partial^2 u_i/\partial x_j^2$ will be neglected because it is important only in the laminar sublayer (thickness $\sim$ 1mm) and negligible in the rest of the PBL compared with the eddy diffusion that will appear later in the equations. The same argument is applied in the thermodynamic equation to neglect the term $\chi_T \partial^2\theta/\partial x_j^2$

Then, the set of equations takes the form:

$$\frac{\partial u_i}{\partial t} + u_j \frac{\partial u_i}{\partial x_j} = -\frac{1}{\rho}\frac{\partial p}{\partial x_i} - g\,\delta_{3i} - \varepsilon_{ijk}\, f_j\, u_k \qquad (2.1.3)$$

$$\frac{\partial \theta}{\partial t} + u_j \frac{\partial \theta}{\partial x_j} = 0 \qquad (2.1.4)$$

To introduce the eddy diffusivities it is necessary to develop the Reynolds equations. This will not be done in detail here (see Busch 1973), but the basic concepts are the following:

Any time dependant variable, say a, can be divided into two parts, one mean value, $\overline{a}$, averaged in a time interval, plus a deviation, a', from that mean value

$$a = \overline{a} + a'$$

where a represents any instantaneous value and, by definition, $\overline{a'} = 0$, provided $\overline{a}$ is constant in a time interval at least equal to the time interval in which it is defined.

Applying this to u_i, Θ, p and ρ in equations (2.1.3) and (2.1.4) for the total flow, and averaging both equations leads to:

$$\frac{\partial \bar{u}_i}{\partial t} + \bar{u}_j \frac{\partial \bar{u}_i}{\partial x_j} = -\frac{1}{\bar{\rho}} \frac{\partial \bar{p}}{\partial x_i} - g\,\delta_{3i} - \varepsilon_{ijk} f_j \bar{u}_k - \frac{\partial}{\partial x_j}(\overline{u_i' u_j'}) \qquad (2.1.5)$$

$$\frac{\partial \bar{\theta}}{\partial t} + \bar{u}_j \frac{\partial \bar{\theta}}{\partial x_j} = -\frac{\partial}{\partial x_j}(\overline{u_j' \theta'}) \qquad (2.1.6)$$

The additional terms in the right hand side of both equations represent the eddy transport of momentum and heat, respectively. To get (2.1.5), fluctuations in density have been neglected, compared with its mean value. Also, the incompressibility hypothesis has been applied.

The next stage is the closure of the Reynolds equations. In the present model first-order closure K theory, is applied. This assumes that:

$$\begin{aligned} -\overline{u_i' u_j'} &= K_m \frac{\partial \bar{u}_i}{\partial x_j} \\ -\overline{u_j' \theta'} &= K_h \frac{\partial \bar{\theta}}{\partial x_j} \end{aligned} \qquad (2.1.7)$$

As this is a one-dimensional model, dependent on z, horizontal homogeneity of the fluid will be assumed. The term $-1/\rho\ \partial p/\partial x_i$ will be replaced by $\varepsilon_{ijk} f_j u_{gk}$, by invoking the geostrophic approximation. Rearranging (2.1.5) and (2.1.6), using (2.1.7) the final expressions for the equations, writing separately both horizontal momentum equations, are obtained:

$$\begin{aligned} \frac{\partial u}{\partial t} &= f(v - v_g) + \frac{\partial}{\partial z}\left(K_m \frac{\partial u}{\partial z}\right) \\ \frac{\partial v}{\partial t} &= -f(u - u_g) + \frac{\partial}{\partial z}\left(K_m \frac{\partial v}{\partial z}\right) \\ \frac{\partial \theta}{\partial t} &= \frac{\partial}{\partial z}\left(K_h \frac{\partial \theta}{\partial z}\right) \end{aligned} \qquad (2.1.8)$$

where the bar over the single variables has been dropped but it is understood that these are the mean values. The horizontal advection terms do not appear in (2.1.8) because of the horizontal homogeneity. The vertical advection term also vanishes because w must be zero at all levels to satisfy the incompressibility of the fluid, since w = 0 necessarily at surface. Thus the term $2 w \Omega \cos(\phi)$ of the u equation also vanishes. The vertical momentum equation is not necessary because, with the assumptions involved, it leads to the hydrostatic approximation.

2.2 Boundary Layer formulations

Two different layers will be considered in the PBL. The first is the surface layer where the fluxes of heat and momentum are constant with height and equal to their values at surface, and where the wind does not change direction with height. The second is the Ekman layer where the fluxes of heat and momentum decrease with height, reaching zero values (by assumption) at the top of the PBL. The wind shifts with height due to decrease of the friction force, and reaches the direction of the geostrophic wind at the top of the PBL.

2.2.1 The constant flux layer

The structure of this layer is relatively well known nowadays, and different researchers have found good agreement between the observations and the formulations of the Monin-Obukhov similarity theory. The theory establishes that the wind shear and temperature gradient can be expressed, respectively, as:

$$\frac{kz}{u_*}\frac{\partial u}{\partial z} = \phi_m \qquad (2.2.1.1)$$

$$\frac{z}{\theta_*}\frac{\partial \theta}{\partial z} = \phi_h \qquad (2.2.1.2)$$

where $\theta_* = \overline{-w'T'}/u_*$

The non-dimensional wind shear, ϕ_m, and the non-dimensional temperature gradient, ϕ_h, introduce the dependence of u and θ on stability conditions within the surface layer. These are universal functions and have been evaluated by Businger et al. (1971):

$$\phi_m = (1-15\zeta)^{-\frac{1}{4}} \qquad \text{for } \zeta<0$$

$$\phi_m = 1+4.7\zeta \qquad \text{for } \zeta>0$$

$$\phi_h = 0.74\ (1-9\zeta)^{-\frac{1}{2}} \qquad \text{for } \zeta<0 \qquad (2.2.1.3)$$

$$\phi_h = 0.74 + 4.7\zeta \qquad \text{for } \zeta>0$$

where $\zeta=z/L$, and L, the Monin-Obukhov length is defined by

$$L=\frac{To\ u^3_{*o}}{kg\ \overline{w'T'}}$$

Equations (2.2.1.1) and (2.2.1.2) may be integrated using the expressions (2.2.1.3), (see Paulson, 1970), obtaining the following:

$$u=\frac{u_*}{k}\ (\ell n\ \frac{z}{zo} - \psi_1) \qquad \text{for } \zeta<0$$

$$u = \frac{u_*}{k}\ (\ell n \frac{z}{zo} + 4.7\zeta) \qquad \text{for } \zeta>0 \qquad (2.2.1.4)$$

$$\theta-\theta_o = 0.74\ \ \theta_*\ (\ell n\ \frac{z}{zo} - \psi_2) \qquad \text{for } \zeta<0$$

$$\theta-\theta_o = 0.74\theta_*(\ell n\ \frac{z}{zo} + 4.7\zeta) \qquad \text{for } \zeta>0$$

where

$$\psi_1 = 2\ \ell n[(1+x)/2] + \ell n[(1+x^2)/2] - 2\ \tan^{-1}x+\frac{\pi}{2}$$

$$\psi_2 = \ell n[(1+y)/2]$$

$$x = (1-15\zeta)^{\frac{1}{4}}$$

$$y = (1-9\zeta)^{\frac{1}{2}}$$

According to the Monin-Obukhov similarity theory the integrated expressions for u and θ are valid when z_o, the roughness parameter, is much less than z. In the present model z_o is .01 m and the expressions are integrated up

to the height of the surface layer which is set equal to 40 m, as will be explained later.

2.2.2 The PBL above the surface layer

In the present model mixing length theory will be invoked, and the formulation for the eddy exchangecoefficient of momentum (following Walmsley, 1972) will be:

$$K_m = \frac{\ell u_*}{\phi_m} \qquad (2.2.2.1)$$

where ℓ, is the mixing length, is

$$\ell = k(z+z_o) \exp(-z/\beta) \qquad (2.2.2.2)$$

and β, the height of the maxima in the coefficients, is specified as .30 the height of the PBL.

The turbulent transfer at all levels in the PBL depends on the surface layer characteristics and these are introduced by u_* and by the factor ϕ_m in the formulation of the eddy exchange coefficient. This formulation of K_m is in close agreement with the polynomial proposed by O'Brien (1970), increasing rapidly with height until its maximum and then decreasing slowly and approaching zero as z tends to infinity. The thermal eddy diffusivity is proposed in a similar manner:

$$K_h = \frac{\ell u_*}{\phi_h} \qquad (2.2.2.3)$$

These formulations for the eddy exchange coefficients will allow the heat transfer to be more efficient than the momentum transfer since:

$$\frac{K_h}{K_m} = \frac{\phi_m}{\phi_h} > 1$$

The inclusion of ϕ_m and ϕ_h in K_m and K_h, respectively will allow them to change as the stability changes. It should be mentioned that in both cases ϕ_m and ϕ_h are evaluated in the surface layer.

The fluxes of momentum for the u and v wind components and sensible heat are represented, respectively, by:

$$-\overline{u'w'} = K_m \frac{\partial u}{\partial z}$$

$$-\overline{v'w'} = K_m \frac{\partial v}{\partial z} \qquad (2.2.2.4)$$

$$-\overline{w'\theta'} = K_h(\frac{\partial \theta}{\partial z} - \gamma_c)$$

where the presence of the term γ_c permits a counter-gradient heat flux as explained below.

In a well-mixed planetary boundary layer, for example in the early afternoon, the vertical profile of potential temperature shows an unstable layer in the lowest levels up to a height about 200 m , induced by the heating from the ground, and a neutral to slightly stable layer above. The sensible heat flux is positive (upward) throughout the PBL. The formulation of a turbulent heat flux proportional, through K_h, to the potential temperature gradient will predict a zero or downward heat flux in the upper part of the PBL in the above described situation. To allow the K-theory to work, it is necessary to introduce a factor γ_c that will allow an upward heat flux throughout the PBL even through layers which are slightly stable. Deardorff (1966) suggested $\gamma_c = 6.5 \times 10^{-4}$ K m^{-1}.

2.3 Numerical Techniques

The model is oriented with its x axis pointing toward the east. The grid consists of 18 points in the vertical. The grid spacing was chosen following the suggestions made by Taylor and Delage (1971) who proposed a log-linear spacing of the vertical coordinate. The grid points are located at the following levels (in m.): 0.1, 11.8, 40, 99, 186, 291, 408, 531, 660, 792, 926, 1062, 1200, 1340, 1480, 1620, 1760 and 1900. In the lower levels the grid spacing follows a logarithmic increment and tends to a constant increment in the upper levels. The first level was chosen as z_o. Also Taylor and Delage proposed the use of a "wall layer" where the flux of momentum is constant. This "wall layer" avoids errors in the wind profile which occur when the finite difference scheme is carried right down to the ground, particularly when the mixing length is proportional to z, as in this model. The height of the "wall layer" is kept constant and equal to 40 m. during the integration and represents the height of the constant flux layer. This is somewhat arbitrary since the height of the constant flux layer changes during the day proportionally to the growing of the planetary boundary layer. This constant height of the "wall layer" may affect the solution.

A forward-in-time and centered-in-space finite difference scheme is used to integrate the model, which is expressed by

$$\frac{\partial u_k}{\partial t} = f\,(v_k - v_g) + \frac{2\,K_{k+\frac{1}{2}}\,(U_{k+1}-U_k)}{(Z_{k+1}-Z_k)\,(Z_{k+1}-Z_{k-1})} - \frac{2\,K_{k-\frac{1}{2}}\,(U_k-U_{k-1})}{(Z_k-Z_{k-1})\,(Z_{k+1}-Z_{k-1})} \qquad (2.3.1)$$

following Estoque and Bhumralkar (1970). A similar expression is used for v and θ. The time step was set equal to 20 seconds according to the com-

putational stability criterion $K \Delta t/\Delta z^2 < .25$, where K represents the maximum of the eddy exchange coefficients.

The values of u, v and θ are defined at the grid points, while the eddy diffusivities, wind shear and temperature gradients are defined at levels halfway between the levels where the temperature and wind components are defined.

2.4 Initialization and Boundary Conditions

The initial potential temperature profile is specified as neutral in the lower levels and an inversion is set in the upper levels. Barotropy is assumed and the geostrophic wind is kept constant during the whole integration period. The surface heat flux is a specified sinusoidal function of the time, with the positive half of the cycle starting at sunrise and with amplitude about 15% the solar constant. The downward heat flux at the top of the PBL is set equal to -.2 of the surface heat flux. This value is somewhat arbitrary, although of the accepted order of magnitude (Deardorff, 1974). With the specified temperature profile constant and no heat flux, the model is integrated until a quasi-steady state for the u and v wind components is reached setting $\phi_m = 1$ according to the neutral conditions. Then, the surface heat flux is introduced and the surface layer is adjusted to the new unstable situation. The surface heat flux and the former u_* defines L and θ_* which are introduced in equations (2.2.1.4) to obtain the new u and θ_o, which in turn define the new u_*. This process marches forward until the solution converges. The temperature profile above the surface layer is kept constant. The new value of ϕ_m defines the new eddy exchange coefficients of momentum which are used to reach the final quasi-steady state for the wind profile. After this, the integration of the model starts.

III TEST OF THE MODEL

The initial conditions for potential temperature is the profile observed at O'Neill, Nebraska, during the Great Plains Experiment, at 0835 CST 25 August 1953 (see Stull, 1973), as shown in Figure 1. The geostrophic wind is assumed to be eastward ($\mu_g = 10$ m s^{-1}, $v_g = 0$). The amplitude of the surface heat flux that gave the best general agreement with the observations was .20 [K m s^{-1}], which corresponds to 14.4% of the solar constant. Busch, Chang and Anthes (1976), using the same data, found the best agreement with an amplitude of .25 [K m s^{-1}]. The potential temperature profiles at 1035, 1235 and 1435 CST, obtained by integrating the model are shown in Figure 2. In general, calculated temperatures differed from observed values (Figure 1) by less than one degree Kelvin. The calculated profiles show (Figure 2) an unstable layer in the low levels, changing to neutral and slightly stable with height. The slightly stable layer produced by the model at 1035 CST just below the inversion, which does not appear later, suggests that the initialization procedure applied must be revised since a neutral temperature profile is not in good agreement with an upward heat flux throughout the PBL and a downward heat just on the top. Obviously, when the integration starts, the levels closer to the upper and lower boundary are heated faster than the levels half way between. Figure 3 shows the observed potential temperature profile compared with the calculated by Busch, Chang and Anthes (1976), and by this model at 1235 CST.

The model fails to treat adequately the cooling above the base of the inversion. The reason may be the somewhat arbitrary upper boundary condition for the thermodynamic equation. In earlier experiments with the model, K

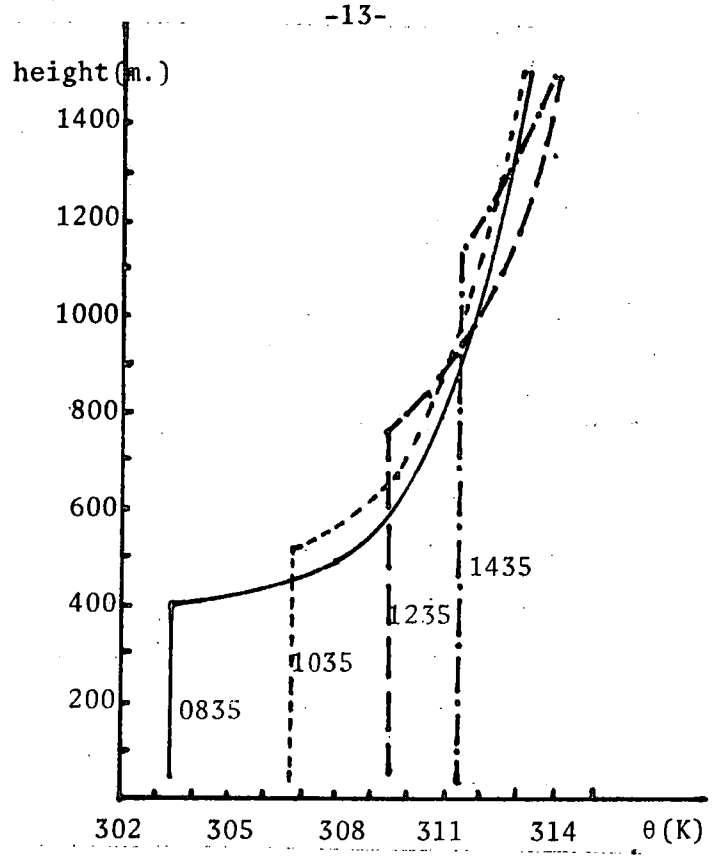

Figure 1. Vertical profiles of potential temperature observed at O'Neill,Nebr. 25 AUGUST 1953 (Stull 1973)

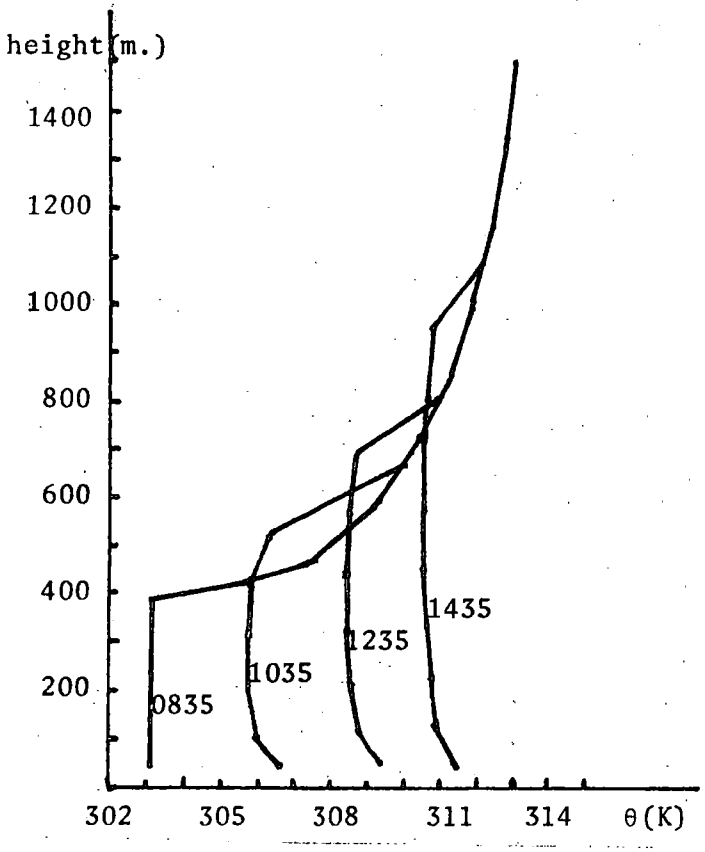

Figure 2. Vertical profiles of potential temperature predicted by the model

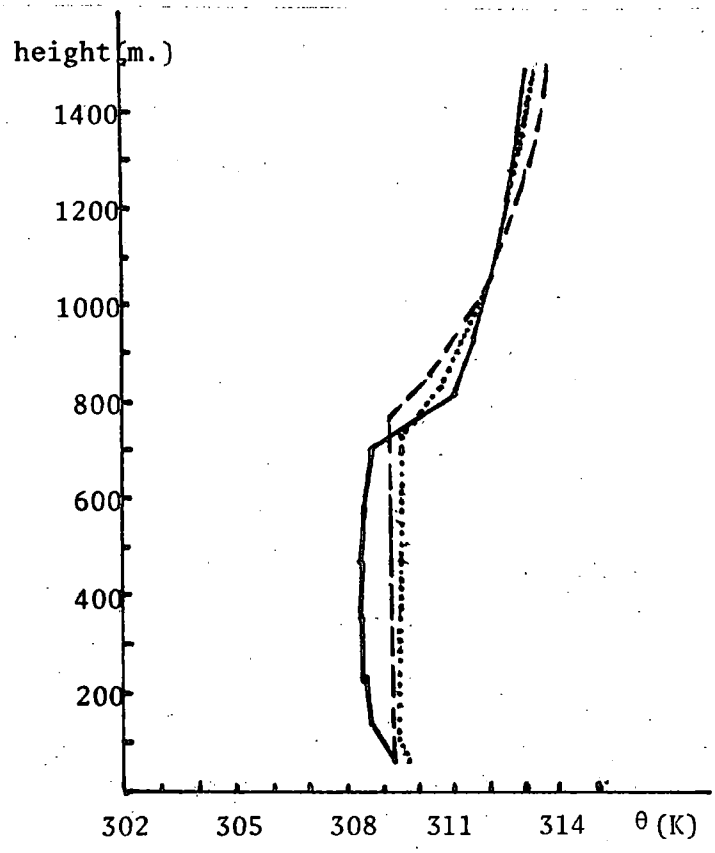

Figure 3. Comparison of the predicted vertical profile of potential temperature (——), with the observed profile (— — —), and the profile predicted by Busch(1976) (.....), at 1235 CST.

theory was employed throughout the vertical domain producing an unrealistic cooling in levels just above the base of the inversion. Hence an unrealistic warming resulted inside the PBL where temperatures deviated from the observations about +4 degrees Kelvin at 1435 CST. This situation probably resulted from the combination of the strong stable lapse rate and slightly excessive K_h values above the PBL, which have almost the same magnitude of those values inside the convective layer, as can be seen in Figure 4b. To overcome this, a downward heat flux was imposed just above the top of the PBL and set equal, in magnitude, to 20% of the surface heat flux while in the rest of the levels above, the heat flux was set equal to zero. Under these assumptions the vertical profiles in Figure 2 were obtained.

This assumption is equivalent, from the point of view of the K-theory, to having vertical profiles of the eddy exchange coefficients as those extrapolated by dashed lines in Figure 4b, approaching small values above the PBL. This should produce smaller downward heat flux inside the inversion, but this has not be tested.

The vertical heat flux profiles shown in Figure 5 are, as expected, decreasing and almost linear functions of height. The imposed downward heat flux just above the PBL represents entrainment of warmer air from the inversion causing local cooling and a warming of the PBL just below the inversion. In Figures 4a and 4b are plotted the vertical profiles of K_m and K_h respectively. The best agreement between the calculated and observed potential temperature profiles was found with $\beta = .5h$ in equation (2.2.2.2) (i.e., the maxima in the eddy exchange coefficients are at half the height of the PBL).

The height of the PBL was defined at every timestep as the height of the inversion base. In Figure 6 has been plotted the time variation of the height of the PBL (dashed line)while dots represent the observed values

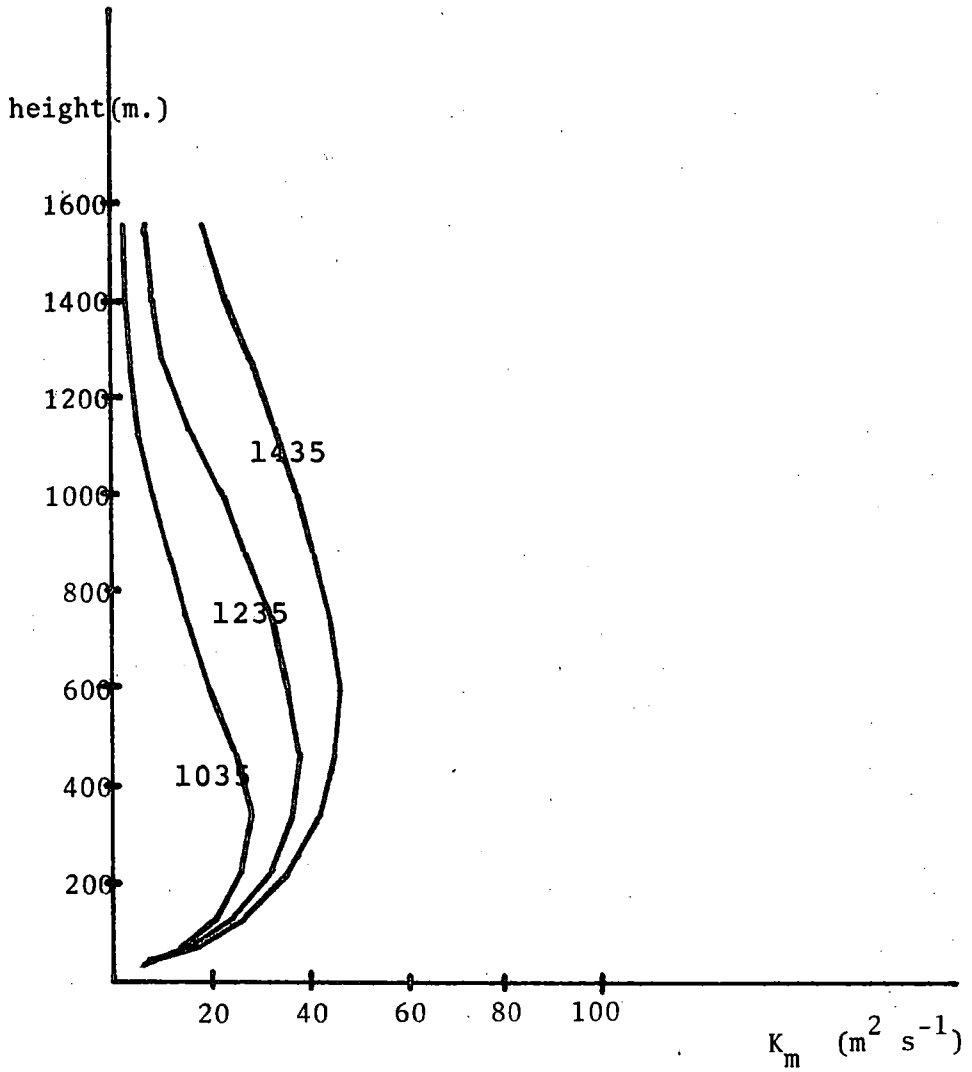

Figure 4a.Vertical profiles of the eddy exchange coefficient of momentum predicted by the model.

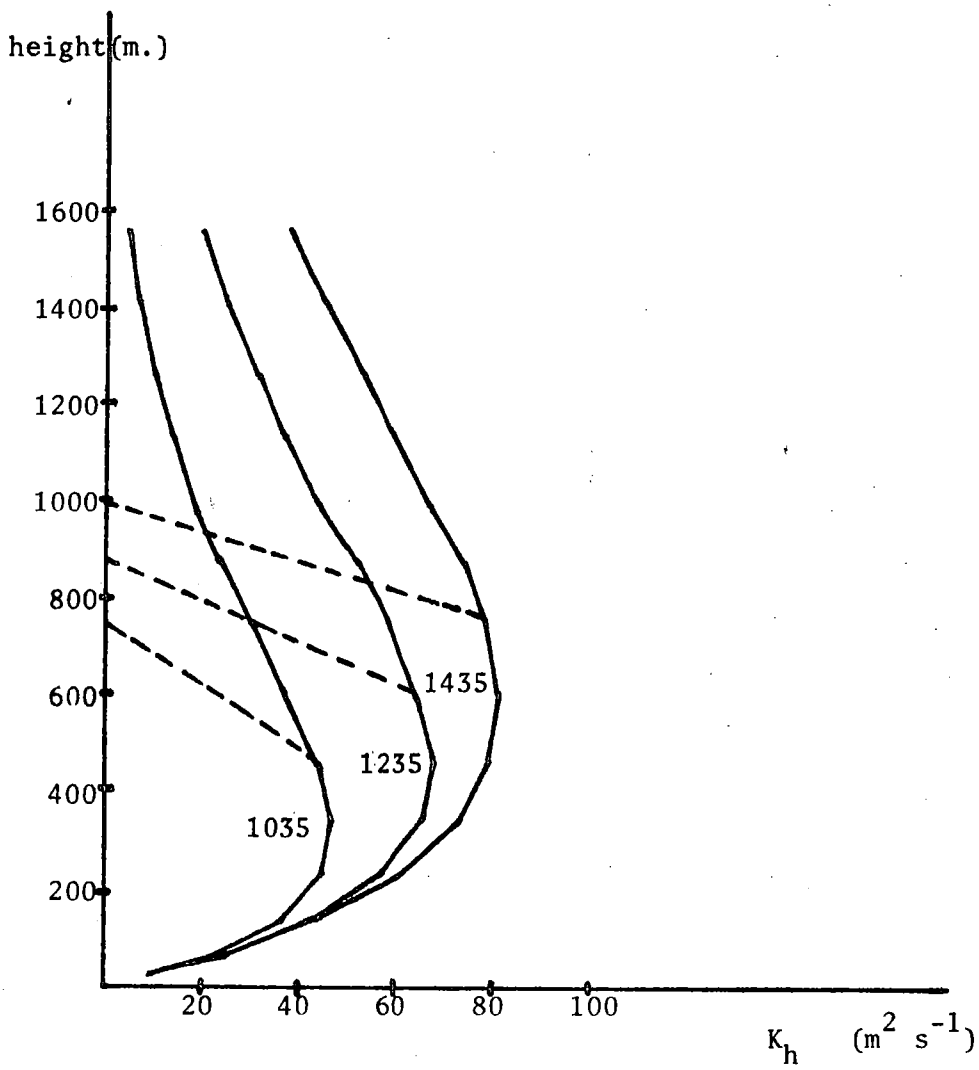

Figure 4b. Vertical profiles of the eddy exchange coefficient of sensible heat predicted by the model. The dashed lines represent the idealized profiles approaching small values just above the top of the PBL.

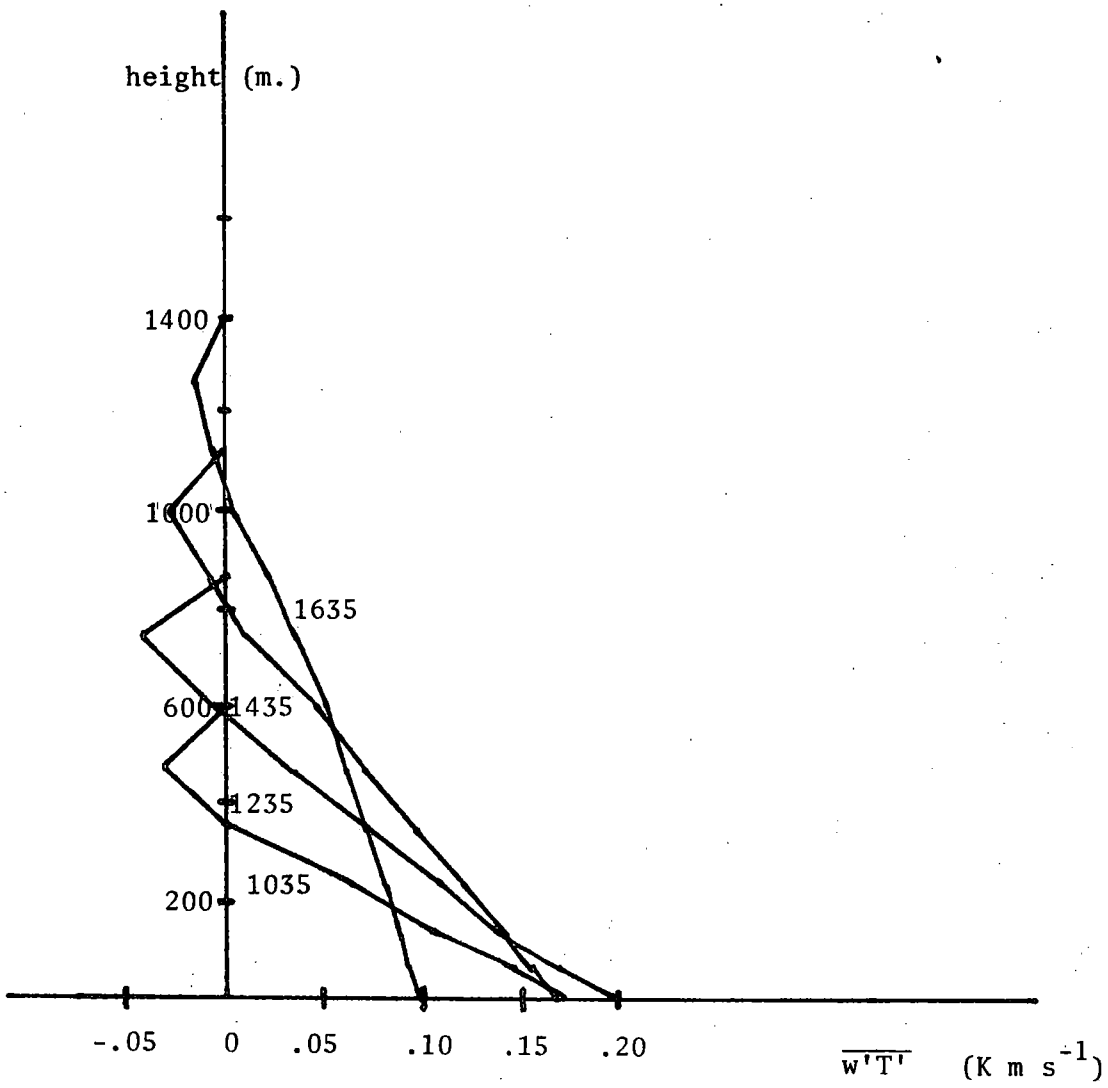

Figure 5. Vertical profiles of sensible heat flux predicted by the model.

(see Stull, 1973). The rate of growing of the PBL is slower specially after 1235 CST and may be due to the smaller cooling predicted just above the PBL. The decaying of the PBL after 1635 CST is not represented by the model; moreover, it predicts a constant increasing PBL at a very slow rate after 1700 CST that is not possible to represent in Figure 6. The reason for that may be the constant cooling predicted by the model above the PBL, while the observed profiles in Figure 1 show heating above 900 m and after 1235 CST, probably due to large scale atmospheric motion.

In Figure 7 are plotted the time variation of the cross isobar flow angle and the magnitude of the wind, both at 11.8 m. Also shown are the results obtained by Busch, Chang and Anthes for the wind at 10 m. As the instability increases the downward momentum flux increases and the wind accelerates and reduces its cross isobar flow angle. In the late afternoon and towards sunset, the instability decreases and the wind decelerates and veers toward larger cross isobar flow angle due to decreased downward momentum flux from the upper levels.

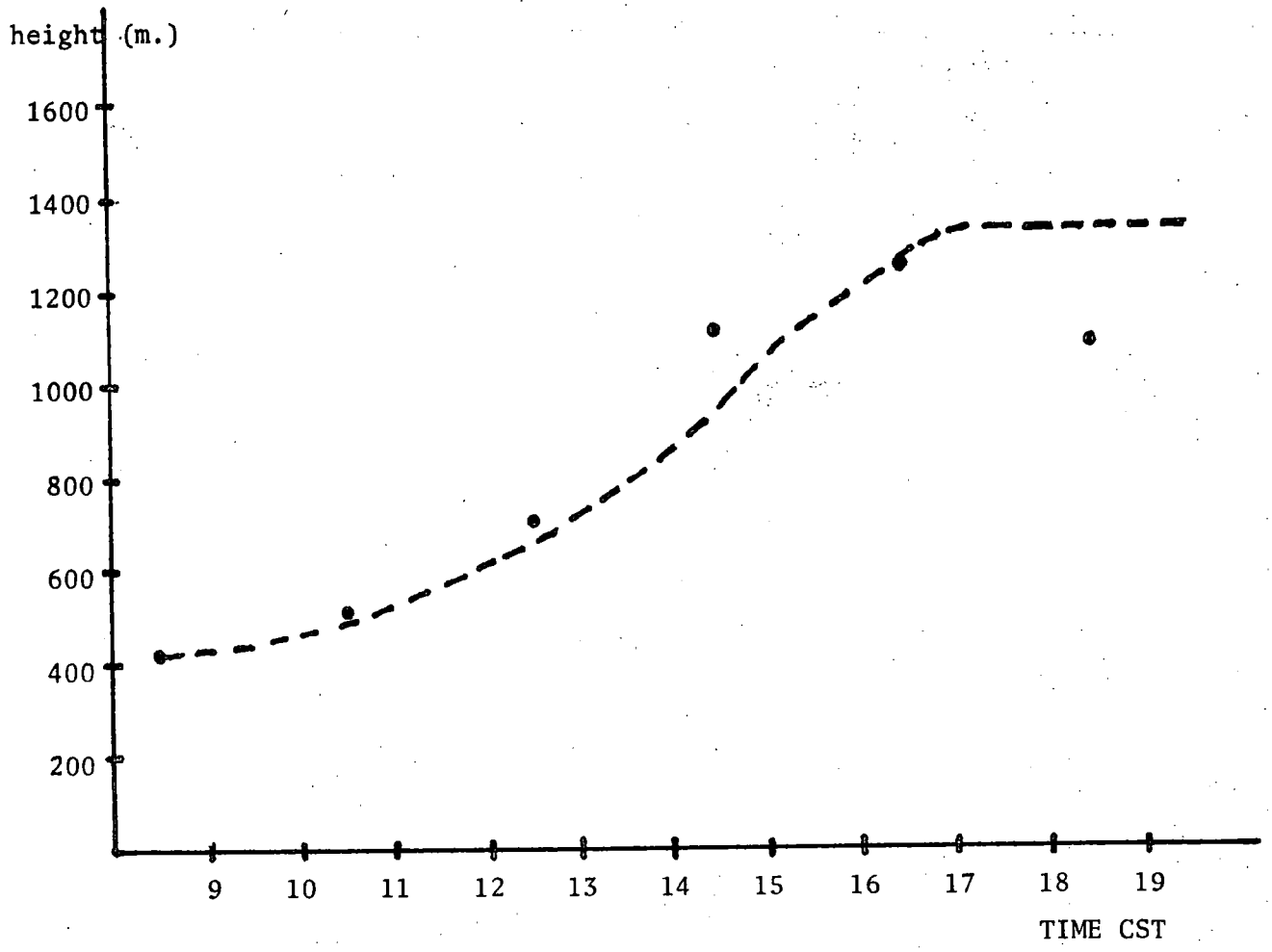

Figure 6. Time variation of the height of the PBL predicted by the model (— — — —). The dots correspond to the observed values (Stull, 1973)

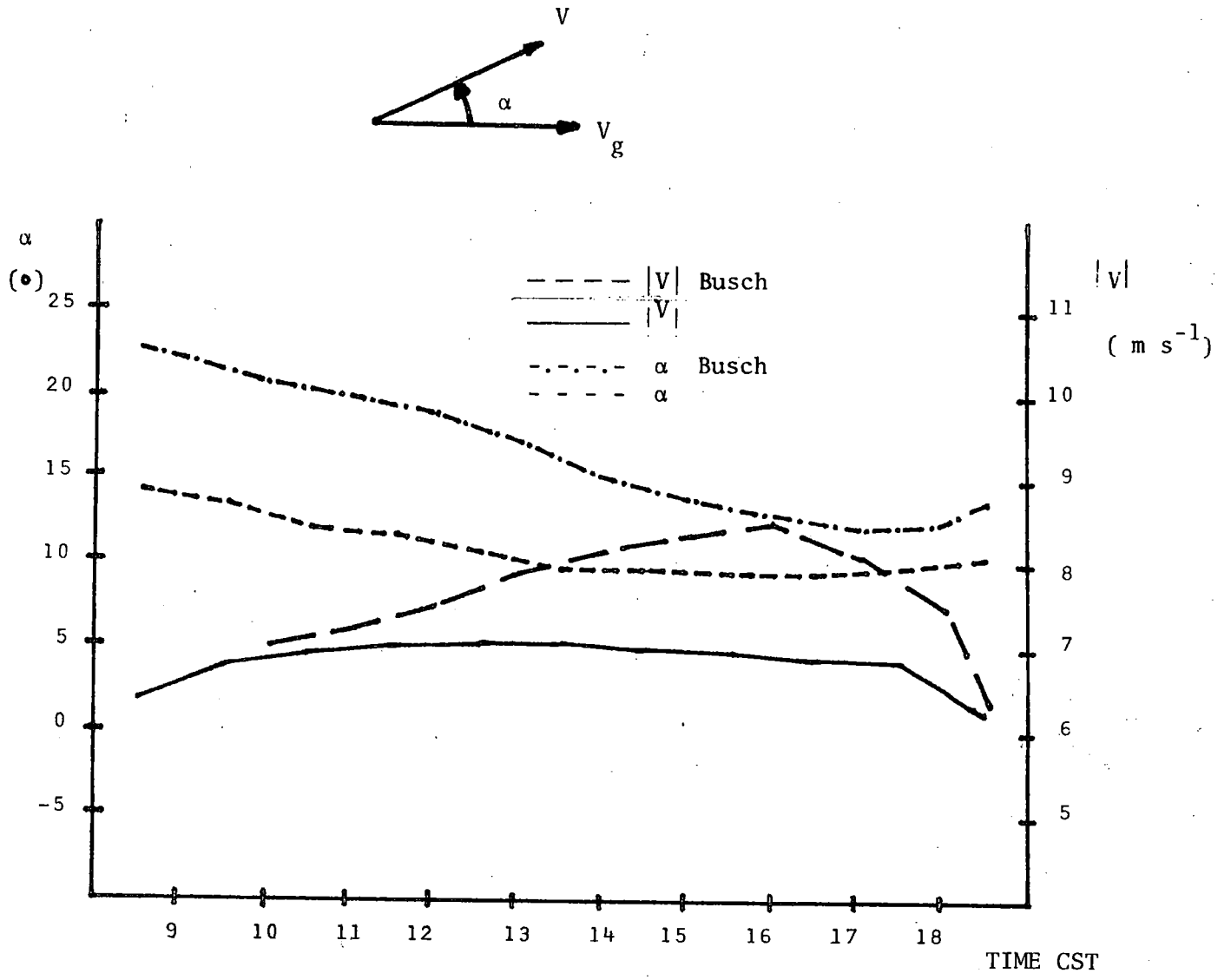

Figure 7. Wind velocity and cross isobar flow angle at 11.8 m predicted by the model, compared with the results of Busch (1976) al 10 m.

IV CONCLUSIONS AND COMMENTS

The model reproduces reasonably well the vertical profiles of potential temperature observed during the Great Plains Experiment on 25 August 1953. Predicted temperatures differed from the observed values by less than one degree Kelvin. The imposed downward heat flux at the base of the inversion causes the model to reproduce qualitatively well the growing of the PBL, although it fails to reproduce the decaying. There is no explicit formulation for the height of the PBL, although this is easily overcome when, as in the present case, the height of thePBL is physically determined by an inversion. The model has not been tested in neutral or slightly stable situations since in this case it would be necessary to specify the height of the PBL, e.g. through Richardson's number considerations or through more elaborated formulations as in Deardorff (1974).

The formulation of the eddy exchange coefficient, and especially K_h, will work better in neutral or slightly stable situations, as discussed in III). In this sense the O'Brien's formulation reproduces better the decaying of K_h close to the upper boundary, moreover, its value at the top of the PBL is specified beforehand and its introduction in the present model is straightforward.

The behaviour of the u and v wind components was not studied in detail, although their behaviour in the surface layer is qualitatively in agreement with the observations.

Finally, it should be mentioned that due to limitations of time available for this project no sensitivity test was made of the numerical techniques and assumptions (e.g. the imposed constant height of the surface layer).

APPENDIX

LIST OF SYMBOLS

a	arbitrary variable
c_p	specific heat for the air, at constant pressure
f_j	each of the coriolis parameters (j = 2,3)
g	gravitational acceleration
h	height of the PBL
k	Von Karman's constant =.35
K	degrees Kelvin
K_h	eddy exchange coefficient of sensible heat
K_m	eddy exchange coefficient of momentum
L	Monin-Obukhov length
L_v	latent heat of evaporation
p	atmospheric pressure
q_s	saturated specific humidity
R_j	radiative heat flux
t	time
T	atmospheric temperature
T_o	temperature of the reference state
u	wind component in the x-direction
u_i, u_j, u_k	each of the wind components (i, j, k = 1,2,3)
u_g	geostrophic wind component in the x-direction
u_*	friction velocity (square root of the friction force per unit mass)
u_{*o}	friction velocity in the constant flux layer
v	wind component in the y-direction

LIST OF SYMBOLS (continued)

v_g	geostrophic wind component in the y-direction
v	wind velocity vector
$\|V\|$	modulus of the wind velocity vector
w	wind component in the z-direction
x_i	each of the rectangular coordinates
z	vertical coordinate
z_o	roughness parameter
α	cross isobar flow angle
β	parameter proportional to the height of the PBL
γ_c	magnitude of the counter-gradient sensible heat flux
δ_{3i}	Kronnecker's delta (δ_{ij}=0 if i≠j and =1 if i=j)
ε_{ijk}	alternating tensor =1 if (i,j,k) = (123), (312) or (231)
	=-1 if (i,j,k) = (321), (213) or (132)
	=0 if i=j or j=k or k=i
θ	potential temperature
θ_o	potential temperature at z_o
θ_*	temperature scale for the surface layer
χ_T	molecular exchange coefficient of sensible heat
ℓ	turbulent mixing length
ν	molecular exchange coefficient of momentum
ρ	density
ϕ	latitude
ϕ_m	non-dimensional wind shear
ϕ_h	non-dimensional lapse rate
ζ	stability parameter, defined as z/L
ψ_1 ψ_2	stability functions
Ω	angular velocity of the earth's rotation

REFERENCES

Busch, N.E. (1973): Turbulent transfer in the atmospheric suface layer. Workshop on Micrometeorology, D.A. Haugen (ed.), Am Met. Soc., Boston, pg 1-65.

Busch, N.E., Chang, S.W. and Anthes, R.A. (1976): A multi-level model of the planetary boundary layer suitable for use with mesoscale dynamic models. Journal of Applied Meteorology, 15, pg 909-919.

Businger, J.A., et al. (1971): Flux profile relationships in the atmospheric surface layer, J. Atmos. Sci., 29, 181-189.

Deardorff, J.W. (1974): Three dimensional numerical study of the height and mean structure of a heated planetary boundary layer. Boundary Layer Meteorology, 7, pg 81-106.

Deardorff, J.W. (1966): The counter-gradient heat flux in the lower atmosphere and in the laboratory. Journal of the Atmospheric Sciences, 23, pg 503-506.

Estoque, M.A. and Bhumralkar, C.M. (1970): A method for solving the planetary boundary layer equations. Boundary Layer Meteorology, 1, pg 169-194.

O'Brien, J.J. (1970): A note on the vertical structure of the eddy exchange coefficient in the planetary boundary layer. J. of Atmospheric Sci., 27, pg 1213-1215.

Paulson, C.A. (1970): The mathematical representation of wind speed on temperature profiles in the unstable atmospheric surface layer. J. of App. Met., 9, pg 857-861.

Stull, R.B. (1973): Inversion rise model based on penetrative convection. Journal of the Atmospheric Sciences, 30, pg 1092-1099.

Taylor, P.A. and Delage, Y. (1971): A note on finite - difference schemes for the surface and planetary boundary layers. Boundary Layer Meteorology, 2, pg 108-121.

Walmsley, J.L. (1972): A one dimensional time dependent air-water boundary layer model. Ph.D. thesis, McGill University, Montreal.